UNIVERSITY OF LEEDS

This is a repository copy of *Characterization of three druggable hot-spots in the Aurora-A/TPX2 interaction using biochemical, biophysical and fragment-based approaches*.

White Rose Research Online URL for this paper:
http://eprints.whiterose.ac.uk/122975/

Version: Accepted Version

1
2
3
4
5
6
7
8
9
10
11
12
13
14
15
16
17
18
19
20
21
22
23
24
25
26
27
28
29
30
31
32
33
34
35
36
37
38
39
40
41
42
43
44
45
46
47
48
49
50
51
52
53
54
55
56
57
58
59
60
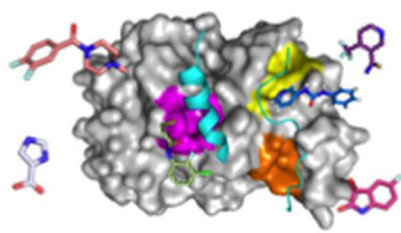
79x39mm (72 x 72 DPI)

Characterization of three druggable hot-spots in the Aurora-A/TPX2 interaction using biochemical, biophysical and fragment-based approaches

Patrick J. McIntyre[1], Patrick M. Collins[2], Lukáš Vrzal[3,4], Kristian Birchall[5], Laurence H. Arnold[5], Chido Mpamhanga[5], Peter J. Coombs[5], Selena G. Burgess[6], Mark W. Richards[6], Anja Winter[1], Václav Veverka[4], Frank von Delft[2,7,8], Andy Merritt[5] and Richard Bayliss[6]

[1]Department of Molecular and Cell Biology, Henry Wellcome Building, University of Leicester, Leicester, LE1 9HN, United Kingdom
[2]Diamond Light Source, Harwell Science and Innovation Campus, Didcot, OX11 0DE, United Kingdom
[3]University of Chemistry and Technology, Technická 5, Prague 6 - Dejvice, Prague, 166 28, Czech Republic
[4]Institute of Organic Chemistry and Biochemistry, Flemingovo nám. 542/2, Prague 6, Prague, 166 10, Czech Republic
[5]LifeArc (Formerly MRC Technology), Stevenage Bioscience Catalyst, Gunnels Wood Road, Stevenage, SG1 2FX, United Kingdom
[6]Astbury Centre for Structural and Molecular Biology, School of Molecular and Cellular Biology, Faculty of Biological Sciences, University of Leeds, Leeds LS2 9JT, United Kingdom
[7]Structural Genomics Consortium, Nuffield Department of Medicine, University of Oxford, Roosevelt Drive, Oxford, OX3 7DQ, UK
[8]Department of Biochemistry, University of Johannesburg, Auckland Park, 2006, South Africa

To whom correspondence should be addressed: Prof. Richard Bayliss, Astbury Centre for Structural and Molecular Biology, School of Molecular and Cellular Biology, Faculty of Biological Sciences, University of Leeds, Leeds LS2 9JT, United Kingdom. E-mail: r.w.bayliss@leeds.ac.uk

ABSTRACT

The mitotic kinase Aurora-A and its partner protein TPX2 (**T**argeting **P**rotein for *Xenopus* kinesin-like protein **2**), are overexpressed in cancers and it has been proposed that they work together as an oncogenic holoenzyme. TPX2 is responsible for activating Aurora-A during mitosis, ensuring proper cell division. Disruption of the interface with TPX2 is therefore a potential target for novel anti-cancer drugs that exploit the increased sensitivity of cancer cells to mitotic stress.

Here, we investigate the interface using co-precipitation assays and isothermal titration calorimetry to quantify the energetic contribution of individual residues of TPX2. Residues Tyr8, Tyr10, Phe16 and Trp34 of TPX2 are shown to be crucial for robust complex

1

formation, suggesting that the interaction could be abrogated through blocking any of the three pockets on Aurora-A that complement these residues. Phosphorylation of Aurora-A on Thr288 is also necessary for high-affinity binding and here we identify arginine residues that communicate the phosphorylation of Thr288 to the TPX2 binding site.

With these findings in mind, we conducted a high-throughput X-ray crystallography-based screen of 1255 fragments against Aurora-A and identified 59 hits. Over three-quarters of these hits bound to the pockets described above, both validating our identification of hot-spots and demonstrating the druggability of this protein-protein interaction. Our study exemplifies the potential of high-throughput crystallography facilities such as XChem to aid drug discovery. These results will accelerate the development of chemical inhibitors of the Aurora-A/TPX2 interaction.

INTRODUCTION

The human kinome contains many sub-families of structurally or functionally related kinases (*1*) such as the Aurora kinases. Aurora-A, B and C are serine/threonine kinases with high sequence similarity within their catalytic domains, yet each plays a different and important role during mitosis (*2*).

During mitosis Aurora-A localises to the poles of the mitotic spindle and along spindle microtubules (*3*). Here it contributes to centrosome separation, assembly of the mitotic spindle and chromosome segregation through phosphorylation of a plethora of substrates (*4, 5*). Owing to its crucial role in many mitotic steps, inhibition of Aurora-A kinase activity can lead to error-prone cell division and cell death (*6*). Aurora-A is frequently overexpressed in cancers and is an attractive target for the development of anti-cancer treatments. Many ATP-competitive inhibitors of the Aurora kinases have been developed but none have been approved for clinical use (*7, 8*).

There are concerns about the selectivity of ATP-competitive Aurora kinase inhibitors due to the similarity between the catalytic domains of the three Aurora kinases. In the case of Aurora-A, this has been addressed by exploiting a single amino acid difference in the active site (*9, 10*). However, an alternative approach to generating Aurora-A inhibitors would be valuable in reducing the risk of off-target kinase inhibition. Kinase inhibitors that act through an allosteric mechanism, such as trametinib, have very high selectivity towards their target (*11*). Though there are currently no potent allosteric inhibitors of Aurora kinases, their development could be envisaged based on knowledge of the regulatory mechanisms of these proteins such as stabilisation of an inactive conformation or disruption of their interactions with upstream activator proteins.

The catalytic activity of Aurora-A is regulated by autophosphorylation on Thr288 and through interactions with protein binding partners such as TPX2 and TACC3 (*12-17*). TPX2 (**T**argeting **P**rotein for ***X****enopus* kinesin-like protein **2**), is the key partner for localising Aurora-A to the mitotic spindle (*15*) and a recent analysis of the co-expression of these two proteins in human cancers suggested that they work together as an oncogenic holoenzyme (*18*). TPX2 also strongly activates Aurora-A, increasing its catalytic activity by at least 7-fold and stimulating autophosphorylation (*13, 14*). In cells, mutation of the TPX2 binding site of Aurora-A reduces activity and causes mislocalisation (*19*). Furthermore, TPX2 protects Aurora-A from dephosphorylation by protein phosphatase 1 (PP1), a function that is abrogated by mutation of TPX2 residue Trp34 (*20*). The minimal binding domain of TPX2 required to interact with Aurora-A is residues 1-43 (*21*). The crystal structure of the Aurora-A/TPX2 complex shows two segments within this region of TPX2 that interact with three hydrophobic pockets on the surface of Aurora-A (Figure 1A). Residues 7-21 of TPX2 adopt an extended conformation that binds to the N-terminal lobe of Aurora-A. Residues 30-43 of TPX2 form an α-helical segment that binds between the N- and C-terminal lobes, near the activation loop, which is phosphorylated on Thr288 (*21*). A recent structure of TPX2 bound to unphosphorylated Aurora-A suggests that only residues 7-21 are required for binding unphosphorylated Aurora-A (*22*).

A compound that blocks the interaction between Aurora-A and TPX2 would disrupt both the localisation and activity of Aurora-A and would be useful in the validation of the Aurora-A/TPX2 complex as a cancer drug target. The identification of 'hot-spots' within a protein-protein interface can help with the search for a protein-protein interaction (PPI) inhibitor (*23*). Hot-spots have been described as clusters of residues that upon loss of functionality (such as through mutation to alanine), cause a significant (at least 2.0 kcal mol^{-1}) change in the binding free energy of a complex (*24-26*). Quantification of the contribution of individual residues to the interaction of TPX2 and Aurora-A would allow greater understanding of the interaction and allow a more targeted, rational approach to blocking the interaction using small molecules.

Here we set out to identify hot-spot residues in the Aurora-A/TPX2 interaction interface, determine the contribution of the α-helical region of TPX2 to the interaction and resolve whether the phosphorylation status of Aurora-A affects the affinity of the interaction. We then conducted an X-ray crystallography-based fragment screen using the XChem facility at Diamond Light Source and identified 59 fragments bound to Aurora-A, the majority of which (46 hits) bound somewhere within the TPX2 binding site. The hot-spots identified in the Aurora-A/TPX2 interface coincide with major sites of fragment binding.

1
2
3
4
5
6
7
8
9
10
11
12
13
14
15
16
17
18
19
20
21
22
23
24
25
26
27
28
29
30
31
32
33
34
35
36
37
38
39
40
41
42
43
44
45
46
47
48
49
50
51
52
53
54
55
56
57
58
59
60

RESULTS and DISCUSSION

Figure 1. Identification of hot-spots in the Aurora-A/TPX2 interface. (A) Crystal structure of Aurora-A (gray, surface) bound to TPX2 (cyan, cartoon, PDB: 1OL5) (*21*). Residues 122-126 of Aurora-A have been removed for clarity. TPX2 residues mutated in this work are coloured purple. The Y-pocket has been coloured yellow, the F-pocket coloured orange and the W-pocket pink. (B) SDS-PAGE analysis of co-precipitation assays. GST is present as an impurity from the production of GST-tagged TPX2. Representative isothermal titration calorimetry (ITC) traces of the binding between Aurora-A^{CA} and TPX2 variants; wild-type (*C*) and F19A (*D*).

Hot-spots in the Aurora-A/TPX2 interface. We initially investigated the contribution of a subset of residues in TPX2 to Aurora-A^{CA} binding using co-precipitation assays (Figure 1B). All tested mutations displayed significantly reduced binding to Aurora-A^{CA} (Table 1, Supporting Information). We then used isothermal titration calorimetry (ITC) to determine the binding affinities of the interactions between Aurora-A and different variants of TPX2. The affinity between Aurora-A^{CA}, phosphorylated on Thr288, and wild-type TPX2 was determined to be 269 nM. As with the co-precipitation assay, all of the mutants tested showed substantially weaker binding to Aurora-A^{CA} than wild type TPX2, ranging from a 6-fold to a 290-fold reduction of binding (Figure 1C, 1D and Table 1). Broadly speaking, the effect of the mutations on TPX2 affinity followed the same trend as seen from the co-precipitation assay. The mutations that had the smallest effect on affinity were D11E, F35A and D11N showing a 6-, 7- and 8.5-fold reduction in binding, respectively. Mutations D11A and F16A had the next most significant effect on binding with 13- and 17-fold reductions in affinity, respectively. However, these translate into differences in the Gibbs free energy change (ΔΔG) of less than 2 kcal mol^{-1} when compared to the wild-type interaction. We therefore do not consider these to be hot-spot residues in the interface, but Phe35 and Phe16 may instead be considered as solvent-occluding 'O-ring' residues adjacent to hot-spot residues. The Asp11 mutations remove a hydrogen bond between this residue in the N-terminal segment of TPX2 and Trp34 the α-helical segment. Binding affinity was affected most significantly by mutations F19A, W34A, Y8A and Y10A which showed reductions of 55-, 59-, 225- and 290-fold, respectively, compared to the native interaction. These correspond to ΔΔG of at least 2 kcal mol^{-1} relative to the native interaction and thus we conclude that Tyr8, Tyr10, Phe19 and Trp34 are hot-spots in the Aurora-A/TPX2 interaction.

4

1
2
3
4
5
6
7
8
9
10
11
12
13
14
15
16
17
18
19
20
21
22
23
24
25
26
27
28
29
30
31
32
33
34
35
36
37
38
39
40
41
42
43
44
45
46
47
48
49
50
51
52
53
54
55
56
57
58
59
60

Table 1. Quantification of the binding of different TPX2 variants to Aurora-A[CA] as determined by co-precipitation and ITC[a]

TPX2 variant	Relative band density	K_a (10^3 M^{-1})	ΔH (kcal mol^{-1})	TΔS (kcal mol^{-1})	ΔG (kcal mol^{-1})	N	K_d (μM)	X-fold reduction in affinity	$\Delta\Delta G$ (kcal mol^{-1})
WT	1.00 ± 0.00	4182.50 ± 635.00	-22.29 ± 0.34	-13.40	-8.88	0.95	0.27 ± 0.04	n/a	n/a
Y8A	/	16.60 ± 1.60	-10.71 ± 3.7	1.62	-1.63	1.36	60.81 ± 5.86	225	7.25
Y10A	0.11 ± 0.07	12.80 ± 0.71	-13.60 ± 0.37	-8.12	-5.48	1.00*	78.37 ± 4.35	290	3.40
D11A	0.48 ± 0.10	276.00 ± 14.00	-13.77 ± 0.11	-6.48	-7.29	0.98	3.63 ± 0.18	13	1.59
D11E	0.65 ± 0.18	611.00 ± 31.00	-32.50 ± 0.28	-24.73	-7.77	0.56	1.64 ± 0.08	6	1.11
D11N	0.66 ± 0.18	439.00 ± 28.00	-4.13 ± 0.05	3.43	-7.56	1.63	2.29 ± 0.15	8.5	1.32
F16A	0.33 ± 0.18	220.00 ± 15.00	-28.75 ± 0.69	-21.59	-7.16	0.45	4.57 ± 0.31	17	1.72
F19A	0.14 ± 0.10	67.90 ± 4.20	-38.35 ± 4.67	-31.94	-6.41	0.39	14.78 ± 0.91	55	2.47
W34A	0.30 ± 0.09	62.90 ± 2.10	-20.70 ± 0.20	-14.24	-6.46	0.86	15.92 ± 0.53	59	2.42
F35A	0.41 ± 0.14	543.00 ± 22.00	-36.24 ± 0.23	-28.51	-7.73	0.54	1.84 ± 0.07	7	1.15

[a]WT, wild-type; K_a, binding constant; ΔH and ΔS, enthalpic and entropic terms; T = 293 K; N, the stoichiometry derived from the curve fitting of each interaction. An asterisk indicates the stoichiometry was fixed at the stated value; K_d, dissociation constant; X-fold reduction in affinity refers to each mutant's K_d value relative to that of WT TPX2; $\Delta\Delta G$, difference in Gibbs' Free Energy change relative to wild-type. For the pull-downs, the relative band density values given are the average Coomassie gel band densities of three separate experiments relative to wild-type TPX2. The errors are the standard deviation between these three band density values. For the ITC experiments, the wild-type condition was performed four times and each mutant condition performed once. Errors quoted were given by Origin software upon curve fitting (mutants) or are the averages of the experimental errors given by Origin software for each individual experiment (WT).

TPX2 senses Aurora-A phosphorylation. The α-helical segment of TPX2 contacts the activation loop of Aurora-A and stabilises a conformation that buries the phosphorylated side-chain, suggesting that the phosphorylation status of Aurora-A might influence the binding of TPX2 (Supplementary Figure S1A) (*21*). Indeed, the binding affinity between TPX2 and unphosphorylated Aurora-A[CA] was measured to be 9-fold weaker than the affinity between TPX2 and phosphorylated Aurora-A[CA] (Supplementary Figure S1B, S1C, Supplementary Table S1). The phosphorylated side-chain of Thr288 interacts with a cluster of arginine residues, including Arg180 and Arg286, mutation of either of which results in binding affinities that are insensitive to the phosphorylation state of the kinase and similar to that of the unphosphorylated, unmutated kinase (Supplementary Figure S1C, Table S1). To identify which of the regions of TPX2 contributed to sensing the phosphorylation state of Aurora-A, we determined the binding affinities of three TPX2 mutants to dephosphorylated Aurora-A[CA] and compared with their affinities for the phosphorylated kinase (Supplementary Table S2). The binding affinity of TPX2 mutants D11A and F16A for phosphorylated and dephosphorylated Aurora-A[CA] exhibited a similar fold-reduction as wild-type TPX2 (7.8–9.8

fold), suggesting that neither of these residues is involved in TPX2 'sensing' the phosphorylation state of Aurora-A. TPX2 mutant F35A, however, had less than 2-fold difference in binding affinity for phosphorylated of dephosphorylated Aurora-A^{CA}. The crystal structure of TPX2 residues 1-45 bound to unphosphorylated Aurora-A catalytic domain shows no density for the α-helical region of TPX2, consistent with its weak interaction at the W-pocket in the absence of phosphorylation of the activation loop (PDB code 4C3P) (22). Thus, we propose that the α-helical region of TPX2 acts as a sensor for the phosphorylation state of the activation loop of Aurora-A through interaction with the W-pocket.

Aurora-A fragment screening. Having concluded that the Aurora-A/TPX2 interaction could be significantly weakened by perturbing any of the three pockets (Y-, F-, or W-), we accessed the XChem platform at Diamond Light Source with the aim of conducting a fragment screen against Aurora-A to identify compounds bound anywhere along the TPX2 binding site. In total, we soaked 1255 fragments into Aurora-A^{CA}-ADP crystals from two different fragment libraries (*27, 28*); the Diamond-SGC Poised Library (DSPL (*29*)) numbered 255 fragments (at the time of screening) and a commercially available Maybridge set containing 1000 fragments. Our crystals were robust, showing no significant difference in diffraction resolution with an increasing amount of DMSO and so 40 % (the top value tested) was chosen as the working concentration, allowing final fragment soaking concentrations of 200 and 80 mM for the DSPL and Maybridge libraries, respectively. Perhaps because of these high soaking concentrations, some crystals were unsuitable for mounting (either the drop contained heavy precipitate or the crystal showed damage) and so the number of crystals mounted was only 1103. Of those mounted and cryocooled, 944 datasets were collected, with an average resolution of 2.2 Å.

Following data collection, the autoprocessed datasets were analysed with the program PanDDA (Pan Dataset Density Analysis) (*30*), which identified statistically significant regions of unmodelled electron density in 184 cases. By manual inspection, 59 unique fragments bound at allosteric sites on the Aurora-A surface were confirmed, giving a total hit rate from our screen of 4.7 % (Supplementary Table S3, Figure 2A). In all cases ADP was bound at the active site. 46 of the 59 allosteric hits were bound in the three pockets that comprise the TPX2 binding site on Aurora-A, with the Y-pocket particularly well sampled with 35 hits (59 % of the total and 76 % of the TPX2-relevant hits, Figure 2B). The F-pocket contained 10 hits (17 % of the total, 22 % of TPX2-relevant hits, Figure 2C) and the W-pocket had a solitary binder. The remaining 13 hits (22 % of total) were scattered all around the kinase domain of Aurora-A^{CA}, including one small fragment that appeared to be coordinated to an Mg^{2+} ion within the active site.

Figure 2. Overview of the crystallographic fragment screen. (A) A representative crystal structure of Aurora-A^{CA} (surface, gray) with TPX2 (cyan, cartoon) superposed for illustrative purposes showing the three TPX2-relevant binding sites seen following fragment screening. Most of the 59 hits bound in the Y-pocket (yellow), some bound in the F-pocket (orange) and a single fragment was bound in the W-pocket (pink) with the remaining hits bound elsewhere around the surface of the protein (not shown) (B) View of the Y-pocket. (C) View of the F-pocket. A representative structure of a single fragment bound to Aurora-A^{CA} is used in both cases to illustrate the pocket with the remaining relevant fragments superposed onto the structure to show the dispersion and breadth of different binding modes seen between the hits.

Upon identification of these hits, we triaged the 46 TPX2-relevant fragments down to just 22 for which the binding was then validated with a variety of orthogonal assays. As both of the main binding sites are highly hydrophobic, the first filter we applied during manual inspection of the hits was to prioritise any fragments exhibiting any non-hydrophobic interactions between ligand and protein. The extremely high fragment concentrations used to soak our crystals could have resulted in a number of false positives and so by identifying specific, strong interactions (such as hydrogen bonds, salt bridges, π-stacking and halogen bonds, by eye and with the use of the Web-based Protein-Ligand Interaction Profiler (PLIP) (*31*)) we eliminated any fragments that were most likely to be non-specific because hydrophobicity positively correlates with increased promiscuity of compounds (*32*). We also eliminated any compounds that were not available commercially in the necessary quantities for a reasonable price. The third filter was an assessment of the fragments' drug-like properties and attractiveness from a medicinal chemistry point of view. This triage process left 22 fragments that we repurchased, although we were unable to source the original fragment in two cases (labelled with an asterisk in Table 2) and used a close analogue instead. The first orthogonal validation assay, NMR-STD, confirmed that the majority of the 22 purchased fragments bound to Aurora-A^{CA} with 8 (fragments **1**, **9**, **12**, **13**, **15**, **16**, **19** and **22**) not showing an STD response (Supplementary Figure S2, Supplementary Table S4).

In parallel, we carried out a fragment-based screen of 1000 compounds (a commercially available collection from Maybridge) against Aurora-A^{CA} using NMR-STD. To prevent binding of fragments to the active site, these experiments were carried out in the presence of an ATP-competitive inhibitor, CCT137690 (*33*) and then hits were classified as any fragment showing a reduced STD response in the presence of TPX2, since this would imply competition for the TPX2 binding site. 47 such hits were identified, with decreases in STD response ranging from 88 % to 5 % (Supplementary Figure S3). We selected 5 fragments exhibiting the most significant decreases in STD response. Affinities for Aurora-A^{CA} in the μM-mM range were measured for each of these fragments, both alone and in the presence of CCT137690, suggesting allosteric binding sites for all five (Supplementary Table S5). Four of the five fragments had been included in the X-ray crystallography screen described above without registering as hits, demonstrating the well-known lack of consistency between different screening methodologies (*34*). We attempted to determine their binding sites using X-ray crystallography but despite collecting good quality X-ray datasets from crystals soaked with each of the five compounds, we found no evidence of bound fragments. We therefore decided to focus on the 22 compounds for which crystallographic data were available.

1
2
3
4
5
6
7
8
9
10
11
12
13
14
15
16
17
18
19
20
21
22
23
24
25
26
27
28
29
30
31
32
33
34
35
36
37
38
39
40
41
42
43
44
45
46
47
48
49
50
51
52
53
54
55
56
57
58
59
60

Using ITC, we obtained binding curves for 15 of the 22 fragments with affinities ranging from 15 μM to 3.75 mM (Supplementary Figure S4). The effect of each fragment on the autophosphorylation of Aurora-A^{CA} was then determined (Supplementary Figure S5). In this assay, each fragment was incubated with unphosphorylated Aurora-A^{CA}, TPX2 and ATP for an hour. Using an antibody specific for Aurora-A phosphorylated at Thr288 its activation loop we were able to quantify the effect of the fragments: 3 showed inhibition, 7 showed activation and the remaining 12 fragments showed no significant effect on Aurora-A^{CA} autophosphorylation. Finally we tested the effect of the fragments on the catalytic activity of Aurora-A^{CA} using the ADP-Quest^{TM} assay, which measures turnover of ATP (35). Using this assay in kinetic mode, we determined IC$_{50}$ values for 8 of the 22 fragments against Aurora-A^{CA} alone, ranging between 18 μM and over 2 mM (Supplementary Figure S6). IC$_{50}$ values could not be measured for five of these eight fragments against the Aurora-A^{CA}/TPX2 complex, suggesting the binding site competition from TPX2 in these cases was too great for the fragment to show an effect. In all but one case the fragment IC$_{50}$ was higher against the Aurora-A^{CA}/TPX2 complex than for Aurora-A^{CA} alone, which would be expected for fragments competing for the binding site of a protein with much higher affinity. The TPX2 concentration in this assay was only twice its K$_d$ for Aurora-A (600 nM versus 270 nM) whereas fragment concentrations were up to 100-fold higher, which could explain why IC$_{50}$ values were seen for the fragments against the Aurora-A^{CA}/TPX2 complex when perhaps no binding would have been expected.

Table 2. Summary of binding data collected for the 22 fragments selected for validation following the crystallography-based fragment screen[a]

Frag No.	Pocket	K$_d$ (μM)	IC$_{50}$ (μM)	% Activation		Frag No.	Pocket	K$_d$ (μM)	IC$_{50}$ (μM)	% Activation
1	W	15	18 / 64	69		12	Y	432	245 / †	154
2	F	-	-	106		13	Y	2792	-	108
3	F	-	-	105		14	Y	494	1105 / -	125
4	F	-	† / †	103		15	Y	1821	† / †	108
5	Y	170	899 / -	188		16*	Y	3753	-	88
6	Y	-	† / -	131		17	Y	1665	-	106
7	Y	894	† / -	91		18	Y	410	108 / 107	48
8	Y	1297	† / -	93		19	Y	-	-	111
9	Y	796	-	77		20*	F	619	1302 / †	259
10	Y	-	308 / 425	90		21	Y	681	-	141

9

11	Y	357	407 / †	60		**22**	F	-	-	127

^{a}K$_d$, dissociation constant; IC$_{50}$, the concentration at which half maximal kinase activity was seen; % Activation, the relative band density compared to a DMSO-containing control condition quantified from a Western blot. A dash indicates that no binding (ITC) or inhibition (activity assay) was seen. A cross indicates that the calculated IC$_{50}$ was higher than 2 mM, the highest assay concentration. The first IC$_{50}$ value refers to Aurora-A^{CA} alone and the second to the Aurora-A^{CA}/TPX2 complex. In all ITC experiments, the stoichiometry between fragment and protein (*N*) was fixed upon curve fitting at a value of 1.00, with the exception of fragment **1** for which this did not result in adequate fitting to the data (*N*=0.43:1). All ITC and kinase activity experiments were performed at least in duplicate, the Western blot assay was performed in triplicate. An asterisk next to a Frag No. indicates the purchased fragment used for these assays is a close analogue of the original crystallographic hit.

Fragment **1,** which was the only hit found in the W-pocket, initially appeared to be the most promising hit (Table 2, Figure 3). Located between the catalytically important αC and αE helices, in the centre of the area to which the α-helical domain of TPX2 binds, a pocket in the surface of Aurora-A had opened up to allow the fragment to interact with the usually buried Cys247. Initially we could not fit the fragment into the visible electron density with any confidence and it was only upon recognising that the fragment contained an isothiazolone ring that the binding mode of the fragment became clear. Thiol groups, such as on cysteine side-chains, are able to cleave the N–S bond of thioazolone rings and form a covalent disulfide bond with the new non-cyclic product (Figure 3A) as seen in our structure (Figure 3B) (*36*). Despite strong inhibition of Aurora-A^{CA} in two different assays, a Hill slope gradient of greater than 2 against both Aurora-A^{CA} and the Aurora-A^{CA}/TPX2 complex was observed, possibly indicating aggregation, non-specific binding of the fragment, or activity through binding to multiple sites (*37*). This was also observed in the biochemical assay data associated with some of the other fragments (e.g. **10)** and it is possible that these fragments interact with the ATP binding pocket. However, fragment **1** belongs to a class of well-known 'PAINS' compounds (*38*) and so we decided not to investigate or develop this further.

Figure 3. A thiazoline compoud bound to the W-pocket. (A) Reaction scheme for the formation of a covalent disulphide between fragment **1** and the thiol of Cys247 on Aurora-A. (B) Crystal structure of fragment **1** bound to Aurora-A^{CA} clearly showing the disulphide bond. The side chain of Lys250 has been removed for clarity. The final 2mFo-DFc electron density map is shown as a wire mesh for the fragment and the side chain of Cys247 contoured to 1.0 σ.

The top six fragments (**5**, **11**, **12**, **14**, **18** and **20**) were selected for a competition assay to determine whether they inhibited the interaction between Aurora-A and TPX2 (Figure 4, 5). The affinity of the interaction between Aurora-A^{CA} and TPX2 was measured in the presence of each of the top six fragments at a concentration of 3 or 4 times their K$_d$ values (Figure 5). In all six cases the measured K$_d$ between Aurora-A^{CA} and TPX2 was weakened compared to the affinity in the absence of compound, with or without DMSO. Fragments **12** and **14** had the least effect on the affinity of the Aurora-A^{CA}/TPX2 complex,

fragments **5** and **11** both caused a two-fold reduction in affinity, and fragment 18 incubation caused an approximately 5-fold reduction in affinity. Fragment **20** had the strongest inhibitory effect, a 12.5-fold reduction in affinity between Aurora-A^{CA} and TPX2. Strikingly, the fragment with the greatest effect in this assay was the only one to bind in the F-pocket, but curiously it had the lowest affinity for Aurora-A (Table 2). In contrast, among fragments that bound to the Y-pocket, affinity for Aurora-A was correlated with strength of Aurora-A/TPX2 interaction inhibition, with the exception of fragment **12**. We conclude that the binding mode, as well as the affinity for Aurora-A, determines the effect on the Aurora-A/TPX2 interaction, and that both pockets should be explored further as targets for the development of inhibitors.

Figure 4. The chemical structures of the top 6 hit fragments identified through our high-throughput X-ray crystallography based screen against Aurora-A. The crystal structure (and corresponding PDB accession code) of each fragment bound to Aurora-A is shown with its final 2mFo-DFc electron density map shown as a blue wire mesh contoured at 1.0 σ. The equivalent data for the remaining 16 repurchased fragments is shown in Supporting Information Figure S7.

Figure 5. Determination of the affinity between Aurora-A and TPX2 in the presence of fragments. (A) The K_d values measured by ITC between Aurora-A^{CA} and TPX2 in the presence of buffer alone ('Control'), buffer containing 5 % DMSO ('DMSO') and each of the top 6 fragments at a concentration of 3 or 4 times their K_d value against Aurora-A^{CA}. (B) ITC traces of the binding of Aurora-A^{CA} to TPX2 in the presence of each of the top 6 fragments.

Druggability of Aurora-A/TPX2. Most of the validated fragment hits from our screen bound to the 'Y-pocket', and mutation of the region of TPX2 that complements this pocket (TPX2 mutants Y10A, Y8A) caused the largest loss of affinity for any TPX2 mutant tested. Compounds that bind this pocket and disrupt the interaction with TPX2 have been described by us and others, and targeting this pocket could provide a strategy for the development of Aurora-A/TPX2 inhibitors (*39*). However, the Y-pocket is analogous to the PDK1-interacting fragment (PIF) pocket, an important regulatory site in the AGC family of kinases (*40*). It is therefore critical to investigate what degree of selectivity could be achieved with compounds that bind with high affinity to this site. The base of the pocket is made of a patch of hydrophobic residues with a surrounding 'wall' of charged residues. Most of the hits lie flat above the base of the pocket forming downward hydrophobic contacts, and in some cases groups branch off the core of the compounds and make specific interactions with surrounding residues. Only one or two compounds explore the space past Tyr199 where the hydrophobic groove extends across the back of the kinase towards the 'F-pocket', the second major binding site for fragment hits.

11

The shallow and expansive nature of protein-protein interactions contrasts with the small, deep, well-defined clefts that are ideal binding sites for small molecules, making PPIs challenging targets in drug discovery. (*41*). However, the large number of hits found in both the Y- and the F-pockets from our fragment screen suggests that the PPI between Aurora-A and TPX2 is potentially druggable. From our results, it might appear that the Y- and F-pockets have a higher hit rate than the W-pocket, and therefore present a better opportunity for drug discovery. However, the nature of our screen contained an inherent bias: in the crystal form of Aurora-A^{CA} used, the Y- and F-pockets face a solvent channel, which would allow easy access to these sites for the soaked fragments while the W-pocket, located between the αC and αE helices of Aurora-A, is much closer to a crystal contact position and as such is less accessible. To definitively probe the druggability of this pocket, another crystal form of Aurora-A should be used in which there is unhindered access of solvent to the W-pocket site. The use of X-ray crystallography as the primary screening method in fragment-based drug discovery is dependent for its success on the availability of a crystal form in which the binding site of interest is not occluded by crystal contacts. Another solution to this problem is to use NMR-based fragment screening. Indeed, we identified hits through NMR screening that were validated by ITC, but unfortunately could not be located in a crystal structure.

The compound 'AurkinA' was recently reported as binding to the Y-pocket of Aurora-A (*39*). It was discovered following a fluorescence anisotropy-based screen and subsequent structure-activity-relationship driven optimisation of the original hit compound. It binds to Aurora-A with a K_d of 4 μM, inhibits its kinase activity and mislocalises Aurora-A from the mitotic spindle in HeLa cells in a manner that suggests the compound does abrogate the Aurora-A/TPX2 interaction. The crystal structure of the Aurora-A/AurkinA complex shows the compound bound in the Y-pocket in a different conformation to any of our Y-pocket fragment hits. Rather than laid flat across the floor of the pocket, AurkinA lies upright against the 'back wall'. Overlaying the compound with the structure of TPX2 bound to Aurora-A shows very similar positioning between Tyr8 of TPX2 and a central aromatic ring of AurkinA. A second group has recently reported small molecule inhibitors of the Aurora-A/TPX2 interaction. The three most potent compounds had K_d values against Aurora-A in the 12-15 μM range (*42*). Initially identified through a virtual screen of the interface (focussed on the Y-pocket), binding to Aurora-A was confirmed using surface plasmon resonance and the compounds were shown to compete with TPX2 for binding to the kinase. Collectively, we have demonstrated the feasibility of targeting the Y-pocket of Aurora-A and inhibiting its interaction with TPX2 *in vitro* and *in cellulo*. The breadth of compounds now reported suggests that the Y-pocket is

druggable. In addition, we have reported a number of F-pocket binders and the single W-pocket binder, some of which affect Aurora-A activity. Finding hits in these additional pockets shows the power and sensitivity of X-ray crystallography as a primary fragment screening technique. The top six fragment hits described here have been taken forward for optimisation with the aim of developing a small molecule inhibitor of the Aurora-A/TPX2 interaction. The development of such compounds is a priority to enable validation of the interaction between Aurora-A and TPX2 as a potential drug target in cancer.

METHODS

Full details of methods are provided in the Supplementary Information.

Accession Codes. Protein Data Bank accession codes for the crystal structures of Aurora-ACA in complex with the following fragments: **1 (5ORL), 2 (5ORN), 3 (5ORO), 4 (5ORP), 5 (5ORR), 6 (5ORS), 7 (5ORT), 8 (5ORV), 9 (5ORW), 10 (5ORX), 11 (5ORY), 12 (5ORZ), 13 (5OS0), 14 (5OS1), 15 (5OS2), 16* (5OS3), 17 (5OS4), 18 (5OS5), 19 (5OS6), 20* (5OSD), 21 (5OSE), 22 (5OSF).**

ACKNOWLEDGEMENTS

ASSOCIATED CONTENT

Supporting Information

The Supporting Information is available free of charge on the ACS Publications website at *http://pubs.acs.org*.
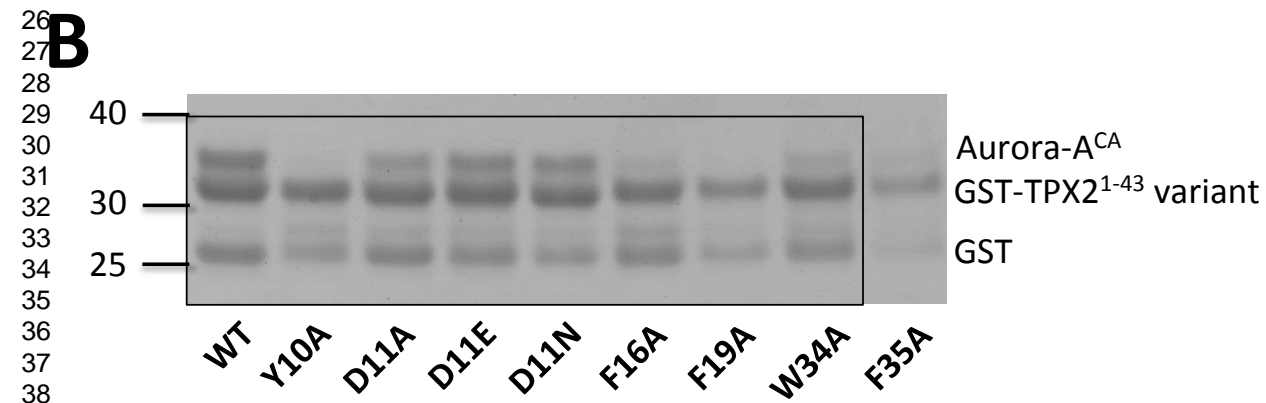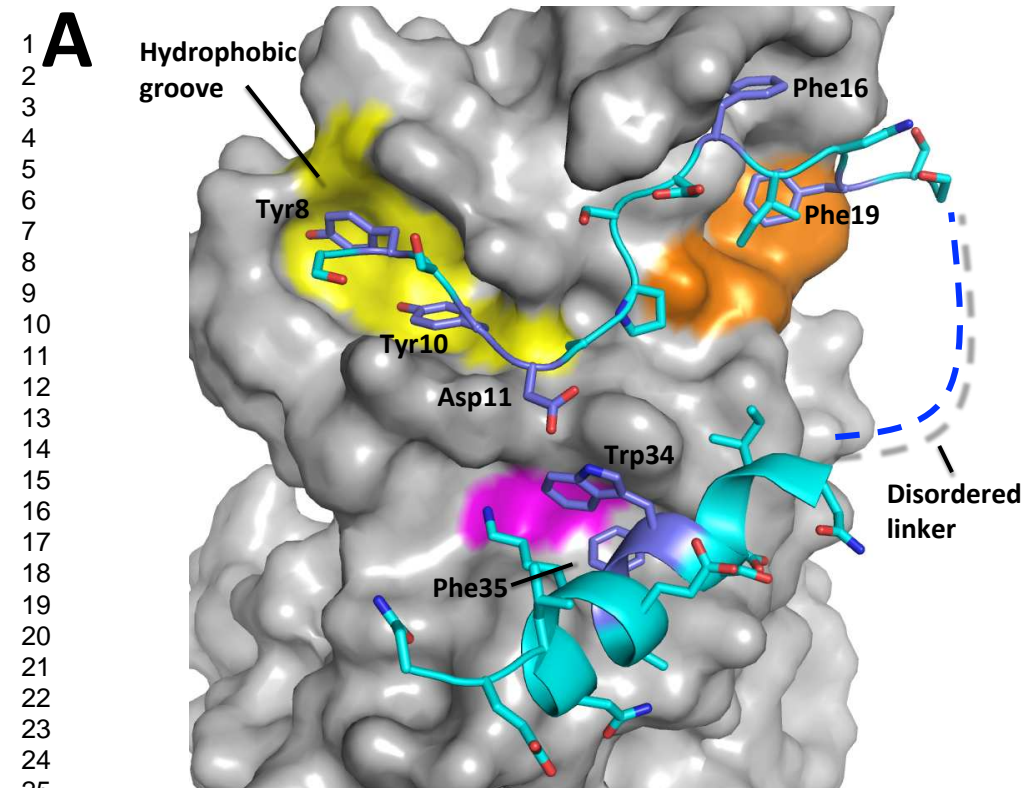
Methods, Tables S1-S5, Figures S1-S7.

Conflict of interest: The authors declare that they have no conflicts of interest with the contents of this article.

13

REFERENCES

1. Manning, G., Whyte, D. B., Martinez, R., Hunter, T., and Sudarsanam, S. (2002) The protein kinase complement of the human genome. *Science 298*, 1912-1934.

2. Carmena, M., and Earnshaw, W. C. (2003) The cellular geography of aurora kinases. *Nat. Rev. Mol. Cell Biol. 4*, 842-854.

3. Roghi, C., Giet, R., Uzbekov, R., Morin, N., Chartrain, I., Le Guellec, R., Couturier, A., Doree, M., Philippe, M., and Prigent, C. (1998) The Xenopus protein kinase pEg2 associates with the centrosome in a cell cycle-dependent manner, binds to the spindle microtubules and is involved in bipolar mitotic spindle assembly. *J. Cell Sci. 111*, 557-572.

4. Giet, R., and Prigent, C. (1999) Aurora/Ipl1p-related kinases, a new oncogenic family of mitotic serine-threonine kinases. *J. Cell Sci. 112*, 3591-3601.

5. Sardon, T., Pache, R. A., Stein, A., Molina, H., Vernos, I., and Aloy, P. (2010) Uncovering new substrates for Aurora A kinase. *EMBO Rep. 11*, 977-984.

6. Manfredi, M. G., Ecsedy, J. A., Meetze, K. A., Balani, S. K., Burenkova, O., Chen, W., Galvin, K. M., Hoar, K. M., Huck, J. J., LeRoy, P. J., Ray, E. T., Sells, T. B., Stringer, B., Stroud, S. G., Vos, T. J., Weatherhead, G. S., Wysong, D. R., Zhang, M., Bolen, J. B., and Claiborne, C. F. (2007) Antitumor activity of MLN8054, an orally active small-molecule inhibitor of Aurora A kinase. *Proc. Natl. Acad. Sci. U. S. A. 104*, 4106-4111.

7. Dar, A. A., Goff, L. W., Majid, S., Berlin, J., and El-Rifai, W. (2010) Aurora kinase inhibitors--rising stars in cancer therapeutics? *Mol. Cancer Ther. 9*, 268-278.

8. Bavetsias, V., and Linardopoulos, S. (2015) Aurora Kinase Inhibitors: Current Status and Outlook. *Front. Oncol. 5*, 278.

9. Bouloc, N., Large, J. M., Kosmopoulou, M., Sun, C. B., Faisal, A., Matteucci, M., Reynisson, J., Brown, N., Atrash, B., Blagg, J., McDonald, E., Linardopoulos, S., Bayliss, R., and Bavetsias, V. (2010) Structure-based design of imidazo[1,2-a] pyrazine derivatives as selective inhibitors of Aurora-A kinase in cells. *Bioorg. Med. Chem. Lett. 20*, 5988-5993.

10. Bavetsias, V., Faisal, A., Crumpler, S., Brown, N., Kosmopoulou, M., Joshi, A., Atrash, B., Perez-Fuertes, Y., Schmitt, J. A., Boxall, K. J., Burke, R., Sun, C., Avery, S., Bush, K., Henley, A., Raynaud, F. I., Workman, P., Bayliss, R., Linardopoulos, S., and Blagg, J. (2013) Aurora isoform selectivity: design and synthesis of imidazo[4,5-b]pyridine derivatives as highly selective inhibitors of Aurora-A kinase in cells. *J. Med. Chem. 56*, 9122-9135.

11. Uitdehaag, J. C., de Roos, J. A., van Doornmalen, A. M., Prinsen, M. B., de Man, J., Tanizawa, Y., Kawase, Y., Yoshino, K., Buijsman, R. C., and Zaman, G. J. (2014) Comparison of the cancer gene targeting and biochemical selectivities of all targeted kinase inhibitors approved for clinical use. *PLoS One 9*, e92146.

12. Littlepage, L. E., Wu, H., Andresson, T., Deanehan, J. K., Amundadottir, L. T., and Ruderman, J. V. (2002) Identification of phosphorylated residues that affect the activity of the mitotic kinase Aurora-A. *Proc. Natl. Acad. Sci. U. S. A. 99*, 15440-15445.

13. Eyers, P. A., Erikson, E., Chen, L. G., and Maller, J. L. (2003) A novel mechanism for activation of the protein kinase Aurora A. *Curr. Biol. 13*, 691-697.

14. Dodson, C. A., and Bayliss, R. (2012) Activation of Aurora-A kinase by protein partner binding and phosphorylation are independent and synergistic. *J. Biol. Chem. 287*, 1150-1157.

15. Kufer, T. A., Sillje, H. H., Korner, R., Gruss, O. J., Meraldi, P., and Nigg, E. A. (2002) Human TPX2 is required for targeting Aurora-A kinase to the spindle. *J. Cell. Biol. 158*, 617-623.

16. Tsai, M. Y., Wiese, C., Cao, K., Martin, O., Donovan, P., Ruderman, J., Prigent, C., and Zheng, Y. (2003) A Ran signalling pathway mediated by the mitotic kinase Aurora A in spindle assembly. *Nat. Cell Biol. 5*, 242-248.

17. Burgess, S. G., Peset, I., Joseph, N., Cavazza, T., Vernos, I., Pfuhl, M., Gergely, F., and Bayliss, R. (2015) Aurora-A-Dependent Control of TACC3 Influences the Rate of Mitotic Spindle Assembly. *PLoS Genet. 11*, e1005345.

18. Asteriti, I. A., Rensen, W. M., Lindon, C., Lavia, P., and Guarguaglini, G. (2010) The Aurora-A/TPX2 complex: a novel oncogenic holoenzyme? *Biochim. Biophys. Acta 1806*, 230-239.

19. Eyers, P. A., and Maller, J. L. (2003) Regulating the regulators: Aurora A activation and mitosis. *Cell Cycle 2*, 287-289.

20. Bayliss, R., Sardon, T., Ebert, J., Lindner, D., Vernos, I., and Conti, E. (2004) Determinants for Aurora-A activation and Aurora-B discrimination by TPX2. *Cell Cycle 3*, 404-407.

21. Bayliss, R., Sardon, T., Vernos, I., and Conti, E. (2003) Structural basis of Aurora-A activation by TPX2 at the mitotic spindle. *Mol. Cell 12*, 851-862.

22. Zorba, A., Buosi, V., Kutter, S., Kern, N., Pontiggia, F., Cho, Y. J., and Kern, D. (2014) Molecular mechanism of Aurora A kinase autophosphorylation and its allosteric activation by TPX2. *Elife 3*, e02667.

23. Guo, W., Wisniewski, J. A., and Ji, H. (2014) Hot spot-based design of small-molecule inhibitors for protein-protein interactions. *Bioorg. Med. Chem. Lett. 24*, 2546-2554.

24. Clackson, T., and Wells, J. A. (1995) A hot spot of binding energy in a hormone-receptor interface. *Science 267*, 383-386.

25. Thorn, K. S., and Bogan, A. A. (2001) ASEdb: a database of alanine mutations and their effects on the free energy of binding in protein interactions. *Bioinformatics 17*, 284-285.

26. Bogan, A. A., and Thorn, K. S. (1998) Anatomy of hot spots in protein interfaces. *J. Mol. Biol. 280*, 1-9.

27. Collins, P. M., Ng, J. T., Talon, R., Nekrosiute, K., Krojer, T., Douangamath, A., Brandao-Neto, J., Wright, N., Pearce, N. M., and von Delft, F. (2017) Gentle, fast and effective crystal soaking by acoustic dispensing. *Acta Crystallogr. D Struct. Biol. 73*, 246-255.

28. Krojer, T., Talon, R., Pearce, N., Collins, P., Douangamath, A., Brandao-Neto, J., Dias, A., Marsden, B., and von Delft, F. (2017) The XChemExplorer graphical workflow tool for routine or large-scale protein-ligand structure determination. *Acta Crystallogr. D Struct. Biol. 73*, 267-278.

29. Cox, O. B., Krojer, T., Collins, P., Monteiro, O., Talon, R., Bradley, A., Fedorov, O., Amin, J., Marsden, B. D., Spencer, J., von Delft, F., and Brennan, P. E. (2016) A poised fragment library enables rapid synthetic expansion yielding the first reported inhibitors of PHIP(2), an atypical bromodomain. *Chemical Science 7*, 2322-2330.

30. Pearce, N. M., Krojer, T., Bradley, A. R., Collins, P., Nowak, R. P., Talon, R., Marsden, B. D., Kelm, S., Shi, J., Deane, C. M., and von Delft, F. (2017) A multi-crystal method for extracting obscured crystallographic states from conventionally uninterpretable electron density. *Nat. Commun. 8*, 15123.

31. Salentin, S., Schreiber, S., Haupt, V. J., Adasme, M. F., and Schroeder, M. (2015) PLIP: fully automated protein-ligand interaction profiler. *Nucleic Acids Res. 43*, W443-447.

32. Leeson, P. D., and Springthorpe, B. (2007) The influence of drug-like concepts on decision-making in medicinal chemistry *Nat. Rev. Drug Discov. 6*, 881-890.

33. Bavetsias, V., Large, J. M., Sun, C., Bouloc, N., Kosmopoulou, M., Matteucci, M., Wilsher, N. E., Martins, V., Reynisson, J., Atrash, B., Faisal, A., Urban, F., Valenti, M., de Haven Brandon, A., Box, G., Raynaud, F. I., Workman, P., Eccles, S. A., Bayliss, R., Blagg, J., Linardopoulos, S., and McDonald, E. (2010) Imidazo[4,5-b]pyridine derivatives as inhibitors of Aurora kinases: lead optimization studies toward the identification of an orally bioavailable preclinical development candidate. *J. Med. Chem. 53*, 5213-5228.

34. Wielens, J., Headey, S. J., Rhodes, D. I., Mulder, R. J., Dolezal, O., Deadman, J. J., Newman, J., Chalmers, D. K., Parker, M. W., Peat, T. S., and Scanlon, M. J. (2013) Parallel screening of low molecular weight fragment libraries: do differences in methodology affect hit identification? *J. Biomol. Screen. 18*, 147-159.

35. Charter, N. W., Kauffman, L., Singh, R., and Eglen, R. M. (2006) A generic, homogenous method for measuring kinase and inhibitor activity via adenosine 5'-diphosphate accumulation *J. Biomol. Screen. 11*, 390-399.

36. Crow, W. D., and Leonard, N. J. (1965) 3-Isothiazolone-cis-3-Thiocyanoacrylamide Equilibria1,2. *J. Org. Chem. 30*, 2660-2665.

37. Walters, W. P., and Namchuk, M. (2003) Designing screens: how to make your hits a hit. *Nat. Rev. Drug Discov. 2*, 259-266.
38. Baell, J. B., and Holloway, G. A. (2010) New substructure filters for removal of pan assay interference compounds (PAINS) from screening libraries and for their exclusion in bioassays. *J. Med. Chem. 53*, 2719-2740.
39. Janecek, M., Rossmann, M., Sharma, P., Emery, A., Huggins, D. J., Stockwell, S. R., Stokes, J. E., Tan, Y. S., Almeida, E. G., Hardwick, B., Narvaez, A. J., Hyvonen, M., Spring, D. R., McKenzie, G. J., and Venkitaraman, A. R. (2016) Allosteric modulation of AURKA kinase activity by a small-molecule inhibitor of its protein-protein interaction with TPX2. *Sci. Rep. 6*, 28528.
40. Schulze, J. O., Saladino, G., Busschots, K., Neimanis, S., Suss, E., Odadzic, D., Zeuzem, S., Hindie, V., Herbrand, A. K., Lisa, M. N., Alzari, P. M., Gervasio, F. L., and Biondi, R. M. (2016) Bidirectional Allosteric Communication between the ATP-Binding Site and the Regulatory PIF Pocket in PDK1 Protein Kinase. *Cell Chem. Biol. 23*, 1193-1205.
41. Arkin, M. R., Tang, Y., and Wells, J. A. (2014) Small-molecule inhibitors of protein-protein interactions: progressing toward the reality. *Chem. Biol. 21*, 1102-1114.
42. Asteriti, I. A., Daidone, F., Colotti, G., Rinaldo, S., Lavia, P., Guarguaglini, G., and Paiardini, A. (2017) Identification of small molecule inhibitors of the Aurora-A/TPX2 complex. *Oncotarget 8*, 32117-32133.

1
2
3
4
5
6
7
8
9
10
11
12
13
14
15
16
17
18
19
20
21
22
23
24
25
26
27
28
29
30
31
32
33
34
35
36
37
38
39
40
41
42
43
44
45
46
47
48
49
50
51
52
53
54
55
56
57
58
59
60

A Hydrophobic groove, Tyr8, Tyr10, Asp11, Trp34, Phe35, Phe16, Phe19, Disordered linker

B
40
30
25
Aurora-A^CA
GST-TPX2^1-43 variant
GST
WT Y10A D11A D11E D11N F16A F19A W34A F35A

C
Time (min)
-10 0 10 20 30 40 50 60 70 80 90 100 110 120
μcal/sec
0.1
0.0
-0.1
-0.2
-0.3
-0.4
-0.5
-0.6
kcal/mole of injectant
2
0
-2
-4
-6
-8
-10
-12
-14
-16
-18
-20
0.0 0.5 1.0 1.5 2.0 2.5
Molar Ratio
WT

D
Time (min)
-10 0 10 20 30 40 50 60 70 80 90
μcal/sec
0.2
0.0
-0.2
-0.4
-0.6
-0.8
-1.0
-1.2
-1.4
kcal/mole of injectant
0
-2
-4
-6
-8
-10
-12
-14
-0.5 0.0 0.5 1.0 1.5 2.0 2.5 3.0 3.5 4.0 4.5 5.0 5.5 6.0 6.5 7.0 7.5
Molar Ratio
F19A

A
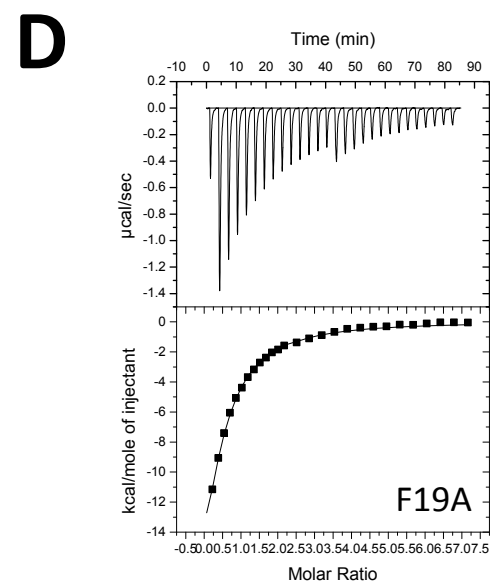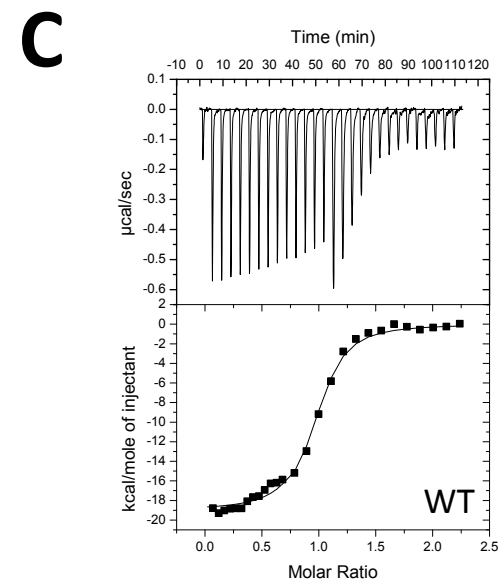
Y-pocket

35 hits

59 %

F-pocket

10 hits

17 %

W-pocket

1 hit

2 %

Elsewhere

13 hits

22 %
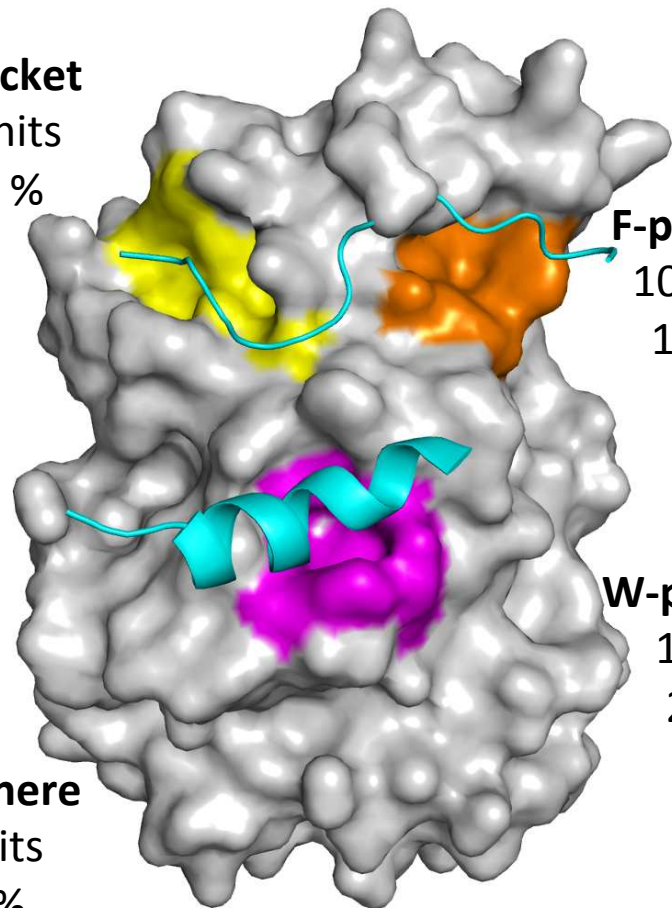
B
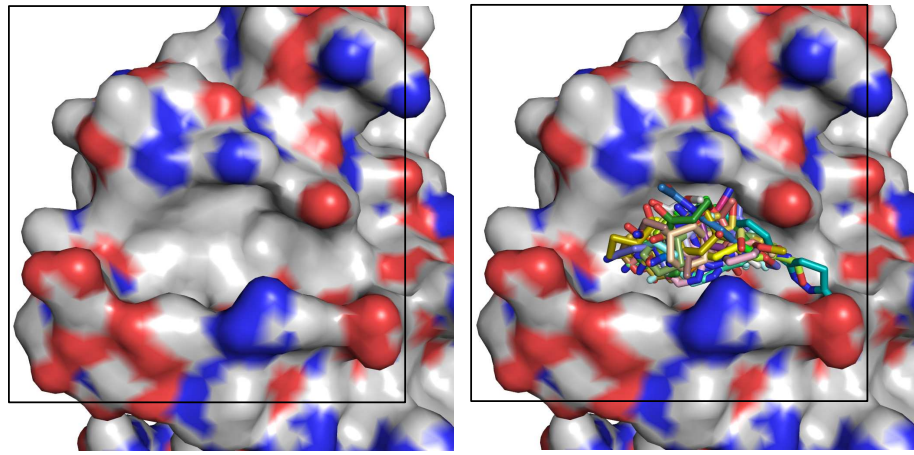
Y-pocket

35 hits
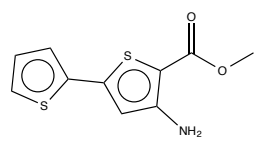
C

F-pocket

10 hits

A

B
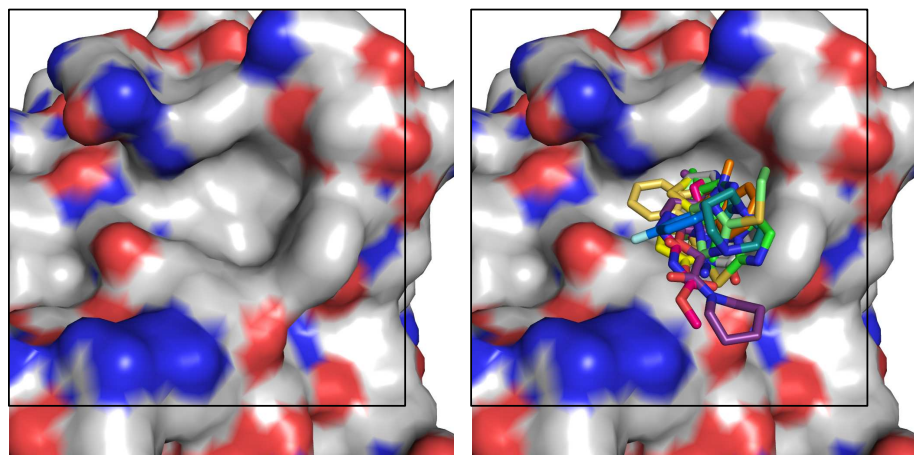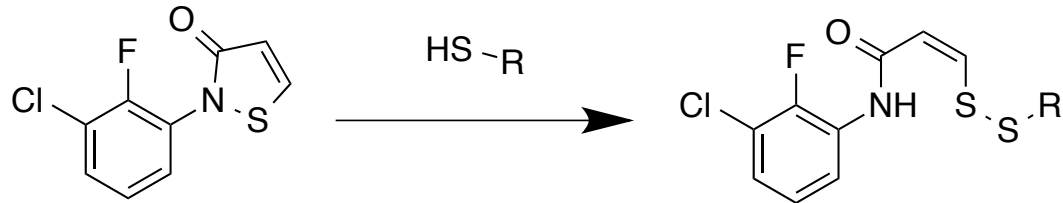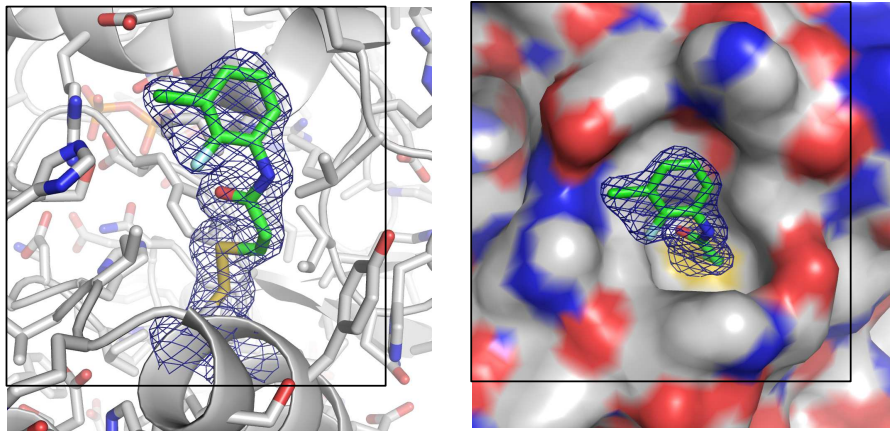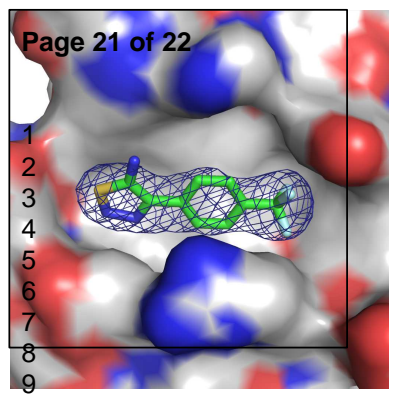
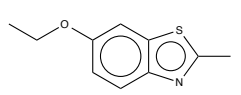Fragment **5**
PDB code: 5ORR
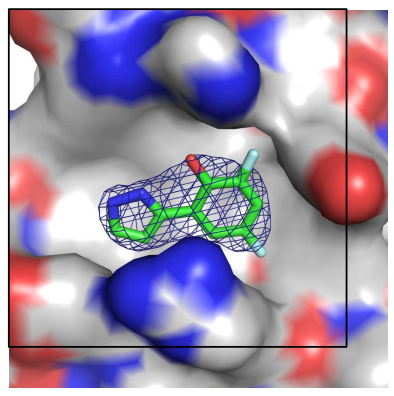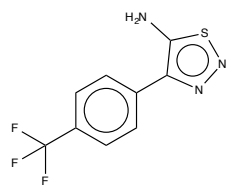
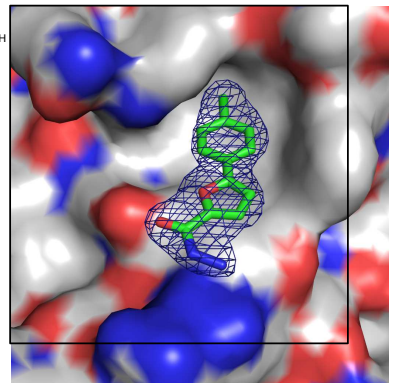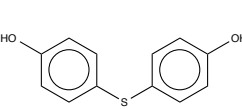Fragment **11**
PDB code: 5ORY
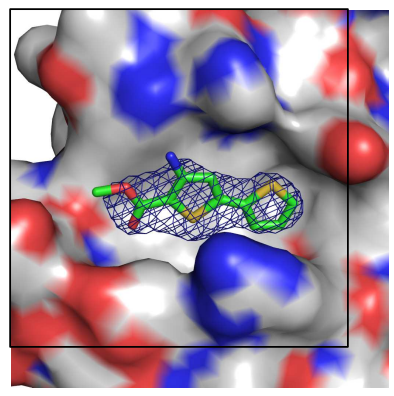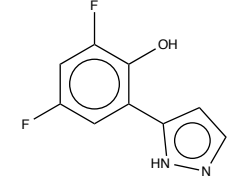
Fragment **12**
PDB code: 5ORZ
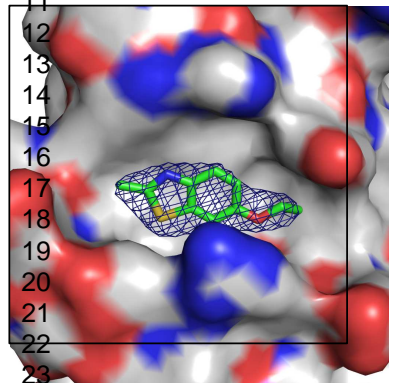
Fragment **14**
PDB code: 5OS1
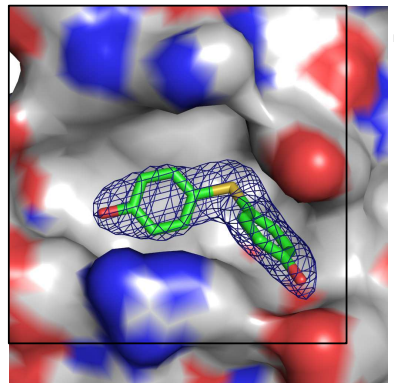
Fragment **18**
PDB code: 5OS5

Fragment **20***
PDB code: 5OSD

1
2
3
4
5
6
7
8
9
10
11
12
13
14
15
16
17
18
19
20
21
22
23
24
25
26
27
28
29
30
31
32
33
34
35
36
37
38
39
40
41
42
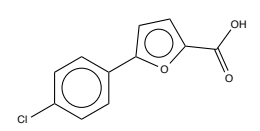
A

		Fragment number						
	Control	DMSO	5	11	12	14	18	20
Aurora-A/TPX2 K_d (µM)	0.27	0.30	0.60	0.62	0.39	0.38	1.39	3.76
Error	0.04	0.06	0.05	0.06	0.04	0.04	0.14	0.51

K_d, dissociation constant measured between Aurora-A and TPX2 by ITC; Error, either the standard deviation between multiple K_d values (control, DMSO) or the error of the fitted curve calculated by Origin software (fragments); Control, the 'standard' affinity between Aurora-A and TPX2; DMSO, in the presence of 5 % DMSO; PM0XX, in the presence of fragment at a concentration of 3/4x its K_d at 5 % final DMSO. Control and DMSO measurements were repeated at least in triplicate, fragment competition measurements were performed once each.

B

5   11   12   14   18   20